Nonsimilar solutions for free convection in non-Newtonian fluids along a vertical plate in a porous medium

Rama Subba Reddy Gorla
Department of Mechanical Engineering, Cleveland State University, Cleveland, Ohio, USA, and
Mahesh Kumari
Department of Mathematics, Indian Institute of Science, Bangalore, India

Received February 1999
Revised May 1999
Accepted July 1999

Keywords *Convection, Boundary layer, Heat transfer, Viscosity index, Porous medium, Vertical plate*

Abstract *A nonsimilar boundary layer analysis is presented for the problem of free convection in power-law type non-Newtonian fluids along a permeable vertical plate with variable wall temperature or heat flux distribution. Numerical results are presented for the details of the velocity and temperature fields. A discussion is provided for the effect of viscosity index on the surface heat transfer rate.*

Nomenclature

f = dimensionless stream function
g = acceleration due to gravity (m/s^2)
h = heat transfer coefficient (W/m^{2}K)
k = thermal conductivity (W/mK)
K = permeability for the porous medium (N m^{n}s^2/kg)
L = plate length (m)
m = consistency index for viscosity (N s^n/m^2)
n = viscosity index
Nu = Nusselt number
Pe = Peclet number
q_w = wall heat flux (W/m^2)
Ra = Raleigh number
T = temperature (K)
u,v = velocity components in x and y directions (m/s)
x,y = axial and normal coordinates (m)
α = effective thermal diffusivity of porous medium (m^2/s)
β = volumetric coefficient of thermal expansion (l/K)
η = similarity variable
θ = dimensionless temperature
ξ = nonsimilar parameter
ρ = density of fluid (kg/m^3)
ψ = stream function

Subscripts
w = wall conditions

Introduction

The porous media heat transfer problem studied in this paper has numerous thermal engineering applications such as geothermal systems, crude oil extraction, thermal insulation and ground water pollution. Cheng and Minkowycz (1977) presented similarity solutions for free convective heat

The authors are grateful to the reviewers whose comments have helped to improve the quality of the paper.

transfer from a vertical plate in a fluid-saturated porous medium. Gorla and co-workers (Gorla and Zinolabedini, 1987; Gorla and Tornabene, 1988) solved the nonsimilar problem of free convective heat transfer from a vertical plate embedded in a saturated porous medium with an arbitrarily varying surface temperature or heat flux. The problem of combined convection from vertical plates in porous media was studied by Minkowycz *et al.* (1985) and Ranganathan and Viskanta (1984). Nakayama and Pop (1985) presented similarity solutions for the free, forced and combined convection. Hsieh *et al.* (1993) derived nonsimilar solutions for combined convection from vertical plates in porous media. Kumari and Gorla (1997) examined the combined convection along a non-isothermal vertical plate in a porous medium. All these studies were concerned with Newtonian fluid flows. A number of industrially important fluids including fossil fuels which may saturate underground beds display non-Newtonian behavior. Non-Newtonian fluids exhibit a nonlinear relationship between shear stress and shear rate.

Chen and Chen (1988) presented similarity solutions for free convection of non-Newtonian fluids over vertical surfaces in porous media. Nakayama and Koyama (1991) studied the natural convection over a non-isothermal body of arbitrary shape embedded in a porous medium.

The present work has been undertaken in order to analyze the free convection from a vertical non-isothermal vertical plate embedded in non-Newtonian fluid-saturated porous media. The boundary condition of variable surface temperature or heat flux is treated in this paper. The power law model of Ostwald de Waele, which is adequate for many non-Newtonian fluids is considered here. The governing equations are first transformed into a dimensionless form and the resulting nonsimilar set of equations is solved by a finite difference method. Numerical results for the velocity and temperature fields are presented.

Analysis

Let us consider the free convention in a porous medium from a permeable vertical plate, which is heated and has a variable wall temperature or heat flux. The properties of the fluid and the porous medium are assumed to be constant and isotropic. The Darcy model is considered which is valid under conditions of small pores of porous medium and flow velocity. The axial and normal coordinates are x and y, and the corresponding flow velocities are u and v respectively. Figure 1 shows the coordinate system and model of the flow. The gravitational acceleration g is acting downwards opposite to the normal coordinate y. The governing equations under the Boussinesq and boundary layer approximations are given by

$$\frac{\partial u}{\partial x} + \frac{\partial v}{\partial y} = 0 \qquad (1)$$

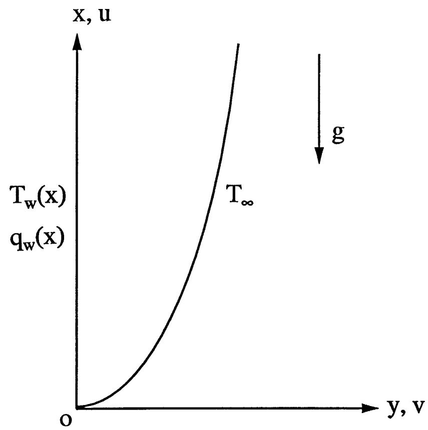

Figure 1.
Coordinate system and flow model

$$u^n = \frac{K}{m}\rho g \beta (T - T_\infty) \tag{2}$$

$$u\frac{\partial T}{\partial x} + v\frac{\partial T}{\partial y} = \alpha\frac{\partial^2 T}{\partial y^2} \tag{3}$$

In the above equations, T is the temperature of the fluid; n is the viscosity index; ρ is the density of the fluid; K is the permeability of the porous medium; β is the volumetric coefficient of thermal expansion; m is the consistency index for viscosity; α is the equivalent thermal diffusivity of the porous medium. With power law variation in wall temperature or heat flux, the boundary conditions can be written as

$$\begin{aligned} &y = 0 : v = V_w, \quad (T - T_\infty) = Ax^\lambda \text{ or } q_w = Bx^\lambda \\ &y = \infty : u = 0, T = T_\infty \end{aligned} \tag{4}$$

It may be shown that if the square of the normal velocity at the wall varies inversely as the distance along the surface (i.e. $V_w \approx x^{-1/2}$), then the problem admits a similarity solution. We note that V_w is a prescribed constant normal velocity at the wall. As shown by Cheng and Minkowycz (1977), the problem becomes similar when $(T_w - T_\infty)$ and q_w are proportional to $x^{-1/2}$. Therefore, values of λ other than –1/2 cannot be analyzed by similarity arguments.

In equation (4), A, B and λ are prescribed constants. Note that $\lambda = 0$ corresponds to the case of uniform wall temperature or heat flux. Although power-law forms are assumed for the wall temperature and heat flux, other types of boundary conditions could be handled by this method. The continuity equation is automatically satisfied by defining a stream function ψ (x,y) such that $u = \frac{\partial\psi}{\partial y}$ and $v = -\frac{\partial\psi}{\partial x}$.

We now define the following dimensionless variables:

$$
\begin{aligned}
&\bar{x} = \frac{x}{L}, \bar{y} = \frac{y}{L} \\
&\bar{u} = \frac{u}{U}, \bar{v} = \frac{v}{U} \\
&U = [\rho g \beta K (T_0 - T_\infty)/m]^{1/n} \\
&Ra = \frac{\rho g \beta K (T_0 - T_\infty) L^n}{m \alpha^n} \\
&Ra^* \ = \ Ra^{1/\mathrm{n}} \\
&\bar{T} = \frac{T - T_\infty}{T_0 - T_\infty} \\
&T_0 = \text{reference \ temperature}
\end{aligned}
\tag{5}
$$

On substituting expressions in equation (5) into equations (1)-(4), we get:

$$\frac{\partial \bar{u}}{\partial \bar{x}} + \frac{\partial \bar{v}}{\partial \bar{y}} = 0 \tag{6}$$

$$(\bar{u})^n = \bar{T} \tag{7}$$

$$\bar{u} \frac{\partial \bar{T}}{\partial \bar{x}} + \bar{v} \frac{\partial \bar{T}}{\partial \bar{y}} = \frac{1}{Ra^*} \frac{\partial^2 \bar{T}}{\partial \bar{y}^2} \tag{8}$$

The boundary conditions may be written as:

$$\bar{y} = 0 : \bar{v} = \bar{V}_w, \bar{T} \approx \bar{x}^\lambda or \frac{\partial \bar{T}}{\partial \bar{y}} \approx -\frac{1}{k} \bar{x}^\lambda \tag{9}$$

In the interest of neatness in presentation, the overbars will be omitted from now on.

A. Variable surface temperature case

Proceeding with the analysis, we define the following transformations:

$$
\begin{aligned}
\eta \ &= \ y x^{\frac{\lambda - n}{2n}} \quad (Ra^*)^{\frac{1}{2}} \\
\psi \ &= \ (Ra^*)^{-\frac{1}{2}} x^{\frac{n+\lambda}{2n}} f(\xi, \ \eta) \\
\xi \ &= \ V_w x^{\frac{n-\lambda}{2n}} (Ra^*)^{\frac{1}{2}} \\
\theta \ &= \ \frac{T}{T_w}
\end{aligned}
\tag{10}
$$

We note that ξ is the surface mass transfer and buoyancy parameter that introduces nonsimilarity into the problem. The governing equations and boundary conditions, equations (6)-(9), can then be transformed into

$$(f')^n = \theta \tag{11}$$

$$\theta'' - \lambda f' \theta + \left(\frac{n+\lambda}{2n}\right) f \theta' = \left(\frac{n-\lambda}{2n}\right)\xi\left[f' \frac{\partial\theta}{\partial\xi} - \theta' \frac{\partial f}{\partial\xi}\right] \tag{12}$$

It may be noted that the governing equations (11) and (12) are nonsimilar (i.e. they depend on ξ and η) because the normal velocity at the wall V_w has been taken as a constant. However, if the normal velocity at the wall $V_w \approx x^{-1/2}$, then the equations (7) and (8) admit a similarity solution and equations (11) and (12) would then depend only on η.

The transformed boundary conditions are given by:

$$\left(\frac{n+\lambda}{2n}\right) f(\xi,0) + \frac{n-\lambda}{2n}\xi\frac{\partial f}{\partial\xi}(\xi,0) = -\xi \text{ or } f(\xi,\ 0) = -\xi, \theta(\xi,0) = 1,$$
$$f'(\xi,\ \infty) = 0\ , \theta(\xi\ ,\ \infty) = 0 \tag{13}$$

The primes in the above equations denote partial differentiations with respect to η. The normal velocity at the wall is suction for negative values of ξ and injection for positive values of ξ.

In the above system of equations, the dimensionless parameter ξ is a measure of the mass transfer and buoyancy effect. Positive values of ξ indicate injection whereas negative values denote suction. Some of the physical quantities of interest include the velocity components u and v in the x and y directions and the local Nusselt number.

The local Nusselt number is given by

$$Nu_x = hx/k \tag{14}$$

where h is the heat transfer coefficient.

The velocity components and Nusselt number are given by:

$$u = x^{\frac{\lambda}{n}} f'(\xi,\eta) \tag{15}$$

$$v = -(Ra^*)^{-\frac{1}{2}} x^{\frac{\lambda-n}{2n}} \left(\frac{n+\lambda}{2n} f(\xi,\eta) + \frac{\lambda-n}{2n}\eta f'(\xi\ ,\eta) + \frac{n-\lambda}{2n}\xi\frac{\partial f}{\partial\xi}\right) \tag{16}$$

$$Nu_x = -(Ra^*)^{\frac{1}{2}} x^{\frac{\lambda+n}{2n}} \theta'(\xi,0) \tag{17}$$

B. Variable surface heat flux case

For this case, the following dimensionless variables are introduced in the transformation:

$$
\begin{aligned}
\eta &= x^{\frac{\lambda-n}{2n+1}} y \\
\xi &= V_w x^{\frac{n-\lambda}{2n+1}} \\
\psi &= x^{\frac{\lambda+n+1}{2n+1}} \mathrm{f}(\xi, \eta) \\
\theta(\xi, \eta) &= \left(\frac{\mathrm{T}}{\mathrm{x}^{\frac{\mathrm{n}(2\lambda+1)}{2n+1}}} \right)
\end{aligned}
\tag{18}
$$

Substituting expressions in equation (18) into the governing equations (6)-(9) leads to

$$
(f')^n = \theta \tag{19}
$$

$$
\theta'' + \frac{\lambda + \mathrm{n} + 1}{2n + 1} \mathrm{f}\theta' - \frac{\mathrm{n}(2\lambda + 1)}{2n + 1} \mathrm{f}'\theta = \frac{\mathrm{n} - \lambda}{2\mathrm{n} + 1} \xi \left[\mathrm{f}' \frac{\partial\theta}{\partial\xi} - \theta' \frac{\partial f}{\partial\xi} \right] \tag{20}
$$

with transformed boundary conditions:

$$
\begin{aligned}
&\frac{(\lambda+\mathrm{n}+1)}{2n+1} \mathrm{f}(\xi,0) + \frac{n-\lambda}{2n+1} \xi \frac{\partial \mathrm{f}}{\partial\xi}(\xi,0) = -\xi \text{ or } \mathrm{f}(\xi,0) = -\xi, \theta'(\xi,0) = -1, \\
&\mathrm{f}'(\xi,\infty) = 0, \quad \theta(\xi,\infty) = 0
\end{aligned}
\tag{21}
$$

and the primes in equations (19)-(21) denote partial differentiations with respect to η.

Note that the ξ parameter here represents the surface mass transfer effect on free convection. Positive values of ξ indicate injection whereas negative values denote suction. The velocity components u and v and the local Nusselt number for this case have the following expressions:

$$
\mathrm{u} = \mathrm{x}^{\frac{2\lambda+1}{2\mathrm{n}+1}} \mathrm{f}' \tag{22}
$$

$$
\mathrm{v} = -\mathrm{x}^{\frac{\lambda-\mathrm{n}}{2\mathrm{n}+1}} \left\{ \frac{\lambda + \mathrm{n} + 1}{2n + 1} \mathrm{f} - p\xi \frac{\partial \mathrm{f}}{\partial\xi} + \frac{\lambda - n}{2n + 1} \cdot \eta f' \right\} \tag{23}
$$

where

$$
p = \frac{n - \lambda}{2n + 1} \tag{24}
$$

$$
\mathrm{Nu_x} = \mathrm{Ra}^{\frac{1}{2}} x^{\lambda+1} / \theta(\xi, 0) \tag{25}
$$

where

$$
\mathrm{Ra} = \frac{\mathrm{L}}{\alpha} \left(\frac{\rho \mathrm{K g} \beta q_w L}{mk} \right)^{1/n} \tag{26}
$$

Numerical scheme

The numerical scheme to solve equations (11) and (12) adopted here is based on a combination of the following concepts:

- The boundary conditions for $\eta = \infty$ are replaced by

$$f'(\xi, \eta_{\max}) = 0, \quad \theta(\xi, \eta_{\max}) = 0 \tag{27}$$

  where $\eta_{\max}$ is a sufficiently large value of η at which the boundary conditions (13) are satisfied. $\eta_{\max}$ varies with the value of n. In the present work, a value of $\eta_{\max} = 25$ was checked to be sufficient for free stream behavior.
- The two-dimensional domain of interest (ξ, η) is discretized with an equispaced mesh in the ξ-direction and another equispaced mesh in the η-direction.
- The partial derivatives with respect to η are evaluated by the second order difference approximation.
- Two iteration loops based on the successive substitution are used because of the nonlinearity of the equations.
- In each inner iteration loop, the value of ξ is fixed while each of the equations (11) and (12) is solved as a linear second order boundary value problem of ODE on the η-domain. The inner iteration is continued until the nonlinear solution converges with a convergence criterion of 10^{-6} in all cases for the fixed value of ξ.
- In the outer iteration loop, the value of ξ is advanced. The derivatives with respect to ξ are updated after every outer iteration step.

In the inner iteration step, the finite difference approximation for equations (11) and (12) is solved as a boundary value problem. We consider equation (11) first. By defining $f = \phi$, equation (11) may be written in the form

$$a_1\phi' + b_1\phi = S_1 \tag{28}$$

where

$$\begin{aligned} a_1 &= (\phi')^{n-1} \\ b_1 &= 0 \\ S_1 &= \theta \end{aligned} \tag{29}$$

The coefficients a_1, b_1 and the source term in equation (28) in the inner iteration step are evaluated by using the solution from the previous iteration step. Equation (28) is then transformed to a finite difference equation by applying the central difference approximations to the first and second derivatives. The finite difference equations form a tridiagonal system and can be solved by the tridiagonal solution scheme.

Equation (12) is also written as a second-order boundary value problem similar to equation (29), namely

$$a_2\theta'' + b_2\theta' + c_2\theta = S_2 \tag{30}$$

where

$$\begin{aligned} a_2 &= 1 \\ b_2 &= \frac{n+\lambda}{2n}\phi \\ c_2 &= -\lambda\phi' \\ S_2 &= \frac{n-\lambda}{2n}\xi\left[\phi'\frac{\partial\theta}{\partial\xi} - \theta'\frac{\partial\phi}{\partial\xi}\right] \end{aligned} \tag{31}$$

The gradients $\frac{\partial\theta}{\partial\xi}$ and $\frac{\partial\phi}{\partial\xi}$ were evaluated to a first-order finite difference approximation using the present value of ξ (unknown) and the previous value of $\xi - \Delta\xi$ (known), with the unknown present value moved to the left-hand side of equation (30).

	Present results		Chen and Chen	
n	$-\theta'(0)$	$f(\infty)$	$-\theta'(0)$	$f(\infty)$
0.5	0.37681	1.08755	0.3768	1.089
0.8	0.42374	1.42078	0.4238	1.421
1.0	0.44371	1.60878	0.4437	1.618
1.5	0.47520	2.01524	0.4752	2.053
2.0	0.49383	2.31914	0.4938	2.403
2.5	0.50562	2.60277	0.5059	2.728

Table I. Comparison of values of $-\theta'(0)$ and $f(\infty)$ for $\lambda = 0$

	$-\theta'(0)$	
λ	Present results	Hsieh *et al.*
0.0	0.44371	0.4438
0.5	0.77004	0.7704
1.0	0.99998	1.0000

Table II. Comparison of values of $-\theta'(0)$ for n = 1

	$1/\theta(0)$	
λ	Present results	Hsieh *et al.*
–0.5	0.58179	0.5818
0.0	0.77146	0.7715
0.5	0.89980	0.8998
1.0	1.00000	0.9999

Table III. Comparison of values of $1/\theta(0)$ for n = 1

The numerical results are affected by the number of mesh points in both directions. To obtain accurate results, a mesh sensitivity study was performed. After some trials, in the η-direction 190 mesh points were chosen whereas in the ξ-direction, 41 mesh points were used. The tolerance for convergence was 10^{-6}. Increasing the mesh points to a larger value led to identical results, up to seven significant decimal places.

The two systems of partial differential equations (11)-(13) and (19)-(21) have similar form. Thus, they were solved using the procedure described above.

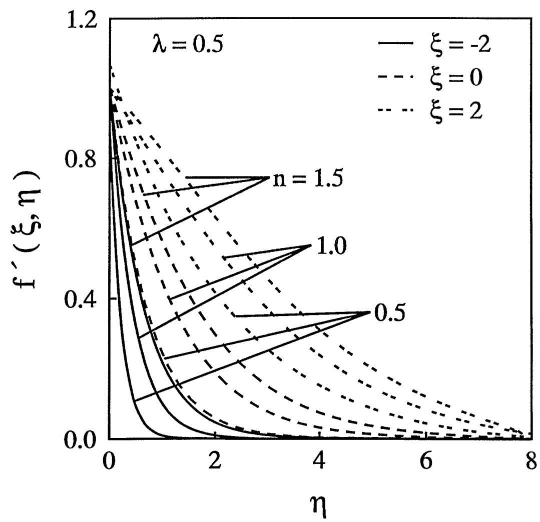

Figure 2.
Velocity profiles for λ = 0.5 (variable surface temperature case)

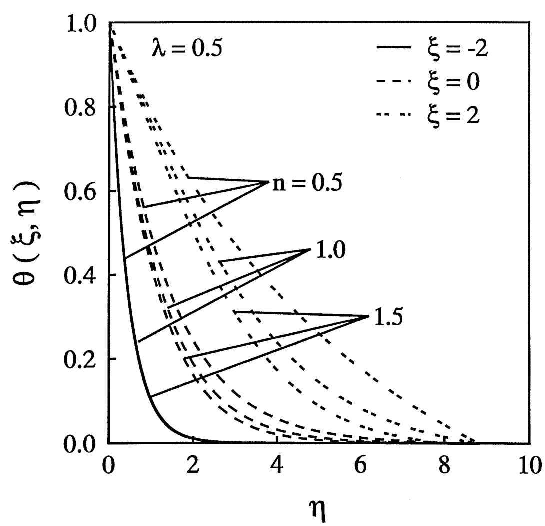

Figure 3.
Temperature profiles for λ = 0.5 (variable surface temperature case)

Results and discussion

Numerical results for $\theta'(\xi, 0)$ and $1/\theta(\xi, 0)$ for the variable surface temperature case and variable surface heat flux case, respectively are tabulated in Tables I, II and III. In order to assess the accuracy of the numerical results, we compare our results for Newtonian fluid (n = 1) with those of Hsieh *et al.* (1993). The agreement between the two is within 0.01 per cent difference. Therefore, the present results are highly accurate.

The velocity and temperature profiles are displayed for the variable surface temperature case in Figures 2, 3, 4, 5 for a range of values of n, λ and ξ. The

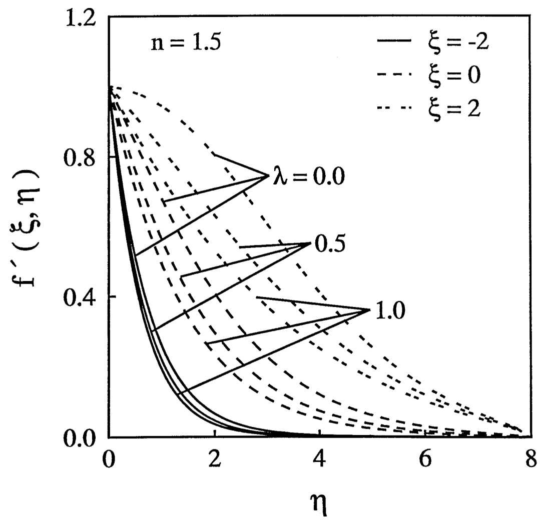

Figure 4.
Velocity profiles for n = 1.5 (variable surface temperature case)

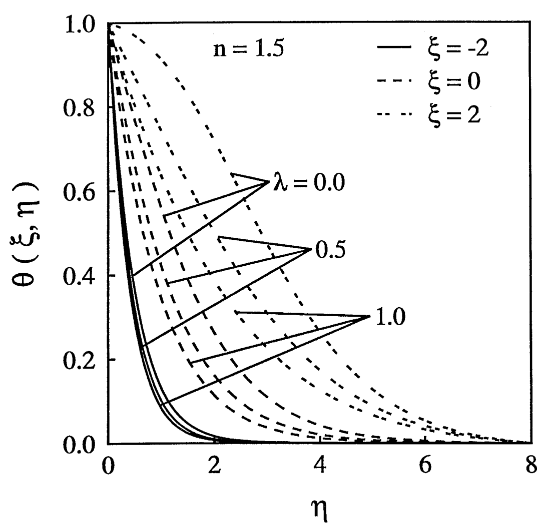

Figure 5.
Temperature profiles for n = 1.5 (variable surface temperature case)

boundary layer thickness decreases as ξ decreases. The slip velocity at the porous surface $f'(\xi, 0)$ increases with the viscosity index n and ξ. The surface temperature gradient and hence the heat transfer rate increase as ξ, n and λ increase.

Figures 6 and 7 display the variation of Nusselt number versus ξ for the variable surface temperature case. Here, n ranged from 0.5 to 1.5 and λ ranged from 0 to 1.5. As λ increases, the Nusselt number increases for a given n. As n increases, the heat transfer rate parameter increases. The effect of surface mass transfer on heat transfer rate will be discussed now. The Nusselt number decreases with injection but the effect of suction is opposite. The thickness of the thermal boundary layer increases with injection but the effect of suction is opposite.

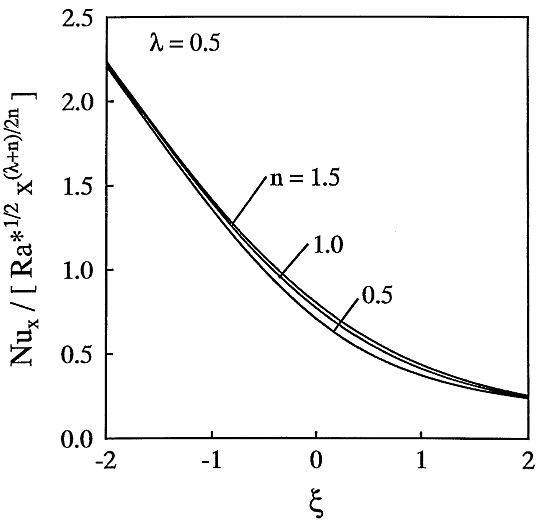

Figure 6. Local Nusselt number versus ξ (variable surface temperature case)

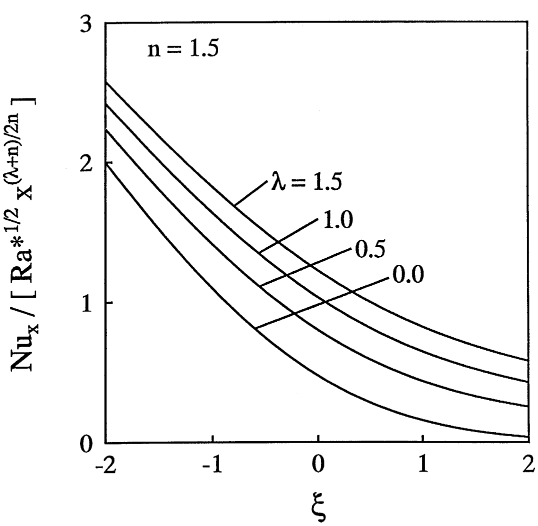

Figure 7. Local Nusselt number versus ξ (variable surface temperature case)

In the interest of conserving space, the velocity and temperature profiles are not presented for the variable surface heat flux case. Figures 8 and 9 display the variation of Nusselt number versus ξ for the variable surface heat flux case. Here, n ranged from 0.5 to 1.5 and λ ranged from 0 to 1.5. As λ and ξ increase, the Nusselt number increases for a given n. As n increases, the heat transfer rate parameter increases.

Concluding remarks

In this paper, we have presented a boundary layer analysis for the free convection in non-Newtonian fluids along a vertical plate embedded in a

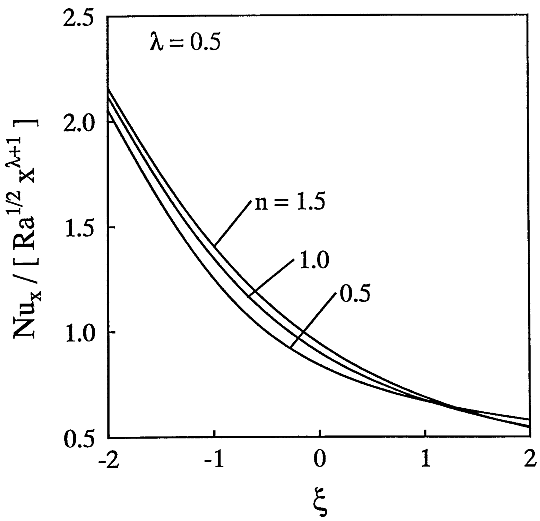

Figure 8.
Local Nusselt number versus ξ (variable surface heat flux case)

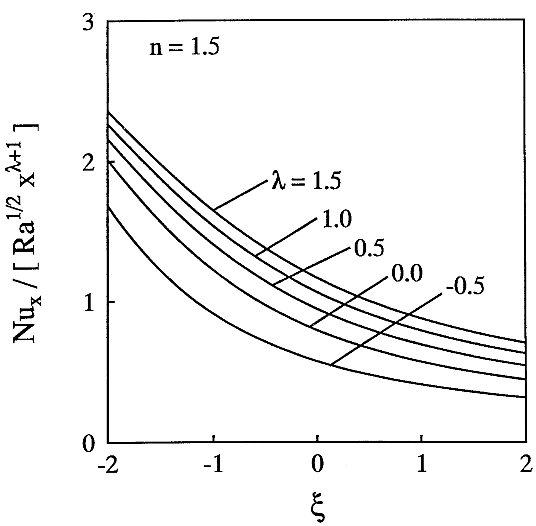

Figure 9.
Local Nusselt number versus ξ (variable surface heat flux case)

fluid-saturated porous medium. Numerical solutions using a finite difference scheme were obtained for the flow and temperature fields for several values of the exponent λ for the surface temperature or heat flux variation and the viscosity index, n.

References

Chen, H.T. and Chen, C.K. (1988), "Free convection of non-Newtonian fluids along a vertical plate embedded in a porous medium", *Transactions of ASME, Journal of Heat Transfer*, Vol. 110, pp. 257-60.

Cheng, P. and Minkowycz, W.J. (1977), "Free convection about a vertical flat plate embedded in a porous medium with application to heat transfer from a dike", *Journal of Geophysical Research*, Vol. 82, pp. 2040-9.

Gorla, R.S.R. and Tornabene, R. (1988), "Free convection from a vertical plate with nonuniform surface heat flux and embedded in a porous medium", *Transport in Porous Media Journal*, Vol. 3, pp. 95-106.

Gorla, R.S.R. and Zinolabedini, A. (1987), "Free convection from a vertical plate with nonuniform surface temperature and embedded in a porous medium", *Transactions of ASME, Journal of Energy Resources Technology*, Vol. 109, pp. 26-30.

Hsieh, J.C., Chen, T.S. and Armaly, B.F. (1993), "Mixed convection along a nonisothermal vertical plate embedded in a porous medium: the entire regime", *International Heat and Mass Transfer Journal*, Vol. 36, pp. 1819-25.

Kumari, M. and Gorla, R.S.R. (1997), "Combined convection along a non-isothermal vertical plate in a porous medium", *Heat and Mass Transfer Journal*, Vol. 32, pp. 393-8.

Minkowycz, W.J., Cheng, P. and Chang, C.H. (1985), "Mixed convection about a nonisothermal cylinder and sphere in a porous medium", *Numerical Heat Transfer*, Vol. 8, pp. 349-59.

Nakayama, A. and Koyama, H. (1991), "Buoyancy-induced flow of non-Newtonian fluids over a non-isothermal body of arbitrary shape in a fluid-saturated porous medium", *Applied Scientific Research*, Vol. 48, pp. 55-70.

Nakayama, A. and Pop, I. (1985), "A unified similarity transformation for free, forced and mixed convection in Darcy and non-Darcy porous media", *International Heat and Mass Transfer Journal*, Vol. 28, pp. 683-97.

Ranganathan, P. and Viskanta, R. (1984), "Mixed convection boundary layer flow along a vertical surface in a porous medium", *Numerical Heat Transfer*, Vol. 7, pp. 305-17.